DESIGN AND SIMULATION OF A BRIDGE-COUPLED DTL STRUCTURE FOR THE 20-80 MeV REGION OF A PROTON LINAC FOR ACCELERATOR TRANSMUTATION OF WASTE*

R. W. Garnett, D. Liska, G. Lawrence, and T. Larkin
Los Alamos National Laboratory
Alamos, New Mexico 87545

Abstract

Recent Los Alamos designs of high-current, CW, proton linacs for accelerator transmutation of waste (ATW) incorporate beam funneling to achieve desired levels of current, emittance, and RF efficiency in the high-beta accelerating structure. Typical designs have a front end consisting of two 350-MHz linacs, each composed of an RFQ and a DTL, accelerating protons to 20 MeV. The two beams are funneled into a 700-MHz CCL which has a final energy in the range 800 to 1600 MeV. The design choice for a 700-MHz accelerating structure in the 20 to 80 MeV region would conventionally be an Alvarez DTL with permanent-magnet quadrupoles (PMQs) in the drift-tubes. However, for high-current, CW, applications, the radiation damage threat from beam loss makes the use of PMQs undesirable, and 700-MHz drift tubes cannot accomodate electromagnet quadrupoles (EMQs). The initial design approach was to begin the 700-MHz CCL structure at 20 MeV. Recent engineering analysis has shown that fabrication of such a structure at low-beta values would be complicated and power efficiency would be low. We have derived a modified DTL concept, the bridge-coupled DTL (BCDTL), that provides an attractive solution for the problem region, with simpler fabrication and higher efficiency.

Introduction

In an earlier linac design for ATW, we proposed a CCL structure from 20 to 1600 MeV. Recently, we have examined the mechanical engineering aspects of such a CCL and have determined that it may be difficult to construct this structure in the 20 to 100 MeV energy region. Because of the difficulties of 1) assembling densely packed cells, 2) power dissipation, 3) the increased possibility of multipactoring for short cells, and 4) poor shunt impedence in this energy range for such a large bore CCL (2.0-2.5 cm radius), we are examining alternative structures for this energy range.

Figure 1 shows a schematic diagram of an ATW type machine. The funneling energy is set at 20 MeV because of increased engineering complexity and stricter beam dynamics requirements at higher energies (higher deflector fields and increased number of funnel components) and the desire to minimize beam-loss-induced activation at the transition region. The ratio of transverse aperture to rms beam size has been used as a figure-of-merit in estimating beam losses. In order to minimize beam loss, we have required this ratio to be 6 or larger throughout the linac, above 20 MeV. This condition requires adequate transverse focusing throughout the linac to maintain beam size and to minimize emittance growth, which could produce beam halo. The ratio of aperture to rms beam size is dependant on the intertank spacing and the type of focusing lattice used. The number of cells per tank of the BCDTL and the transverse phase-advance per focusing period were chosen to optimize the transverse ratio of aperture to rms beam size. However, the magnitude of this ratio is limited by the aperture size, which must be chosen to give reasonable transit-time factors within the cavities.

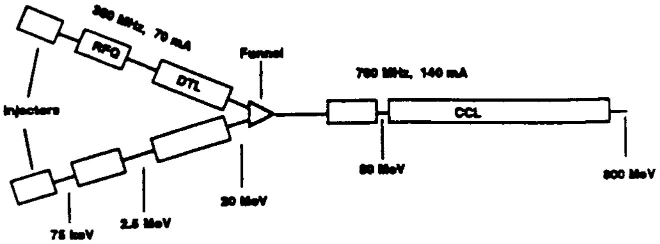

Fig. 1 Schematic Diagram of an ATW-type accelerator. The BCDTL would be used to accelerate the beam from 20 to 80 MeV after the funnel.

Bridge-Coupled DTL Geometry

The BCDTL consists of 86 short, 5-cell drift-tube tanks with EMQs located only between tanks and arranged as a singlet FODO focusing lattice. Each of the tanks is 5-$\beta\lambda$ long and operates at a structure gradient (E_0T) of 1.3 MV/m. This value of structure gradient leads to a constant real-estate gradient of 1 MV/m throughout the BCDTL. This choice of real-estate gradient gives a projected minimum in the accelerator construction cost. The intertank spacing is 2-$\beta\lambda$. Power constraints allow up to four DTL tanks to be bridge-coupled together to make up an RF module. Figure 2 shows, in detail what the BCDTL and module geometry might look like.

Bridge-couplers will be used to couple the TM_{010} accelerating mode into individual tanks. To avoid excessive field droop within individual tanks, when multiple tanks are coupled together, it may be necessary to the couple tanks at the center of each tank as shown in Fig. 2. Coupling at the tank ends would require post couplers for field stabilization.

BCDTL Simulation with PARMILA

The BCDTL was simulated from 20 to 80 MeV as 86 individual tanks with intertank quadrupoles for transverse focusing, using a modified version of the PARMILA code. The PARMILA code was modified for this particular geometry. The equivalent CCL, which also consists of 86 tanks, was also simulated for this energy region using the CCLDYN code. Figure 3 shows the drift-tubes in a tank to all be of equal length, however, they could vary in length as a function of beta as in a typical DTL. In the simulation, the cells were generated in the usual manner, with the drift-tube lengths increasing as a function of beta. Table 1 shows a comparison between the CCL and BCDTL geometry and operating parameters.

---

*Work supported by the US Department of Energy, High Energy and Nuclear Physics Office.

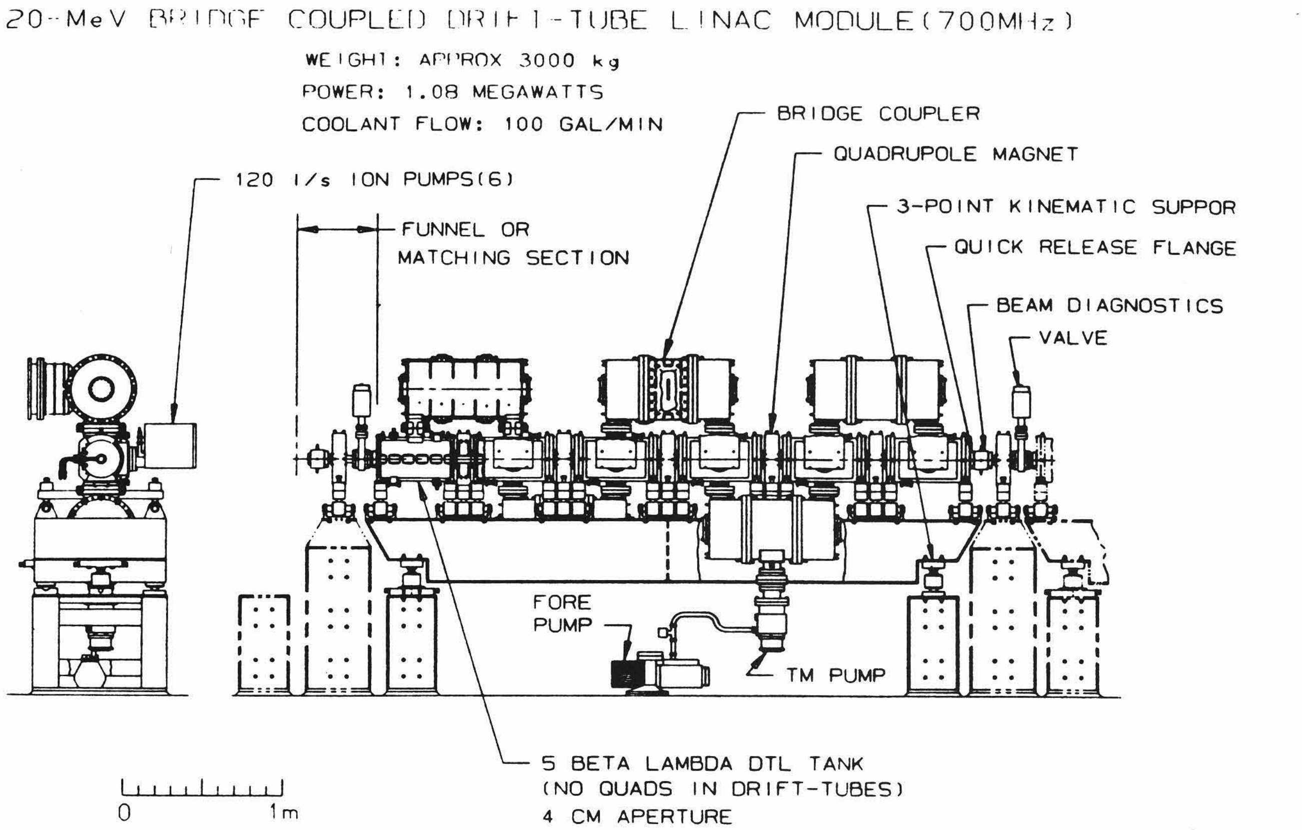

Fig. 2 Conceptual engineering drawing of what a 4-tank module of the BCDTL might look like.

The simulation was run using a fixed transverse aperture radius of 2.0 cm throughout the BCDTL and a beam current of 125 mA. Table 2 summarizes the results of both the BCDTL and CCL simulations. Figure 4 shows the emittance vs cell number for the BCDTL. The beam dynamics results are very similar to those of the CCL design for this energy region. There is essentially no transverse emittance growth. The longitudinal emittance, however, grows because of the constant accelerating gradient. This constant accelerating gradient allows the longitudinal focusing per unit length to become weaker as a function of distance along the linac. Nonetheless, there appears to be no effect of longitudinal emittance growth on the transverse emittance, that could result in a degradation of the ratio of aperture to rms beam size.

Figure 5 shows that, for our chosen aperture, an aperture to rms ratio similar to that of the CCL (10-12.5) is achieved. We have done SUPERFISH calculations which indicate that using the BCDTL structure with a 2.0 cm aperture radius, could lead to approximately a factor of 7 increase in shunt impedance (ZT^2) and reduce the heat load per tank by almost a factor of 6, as compared to a CCL structure. Table 1 also shows the shunt impedence values. The total estimated structure power for the BCDTL (20 to 80 MeV) is 5.1 MW. It should be noted that for this type of application, this structure is heavily beam loaded. The beam power for a beam current of I = 125 mA is 7.5 MW (60% beam loading).

The results of this study indicate that the BCDTL could be a practical alternative to a CCL for the 20 to 100 MeV energy region of an ATW accelerator. This type of structure provides both adequate transverse focusing of high-current beams as needed to control beam-loss-induced structure activation and is electrically efficient in this beta regime.

TABLE 1.

Comparison of CCL and BCDTL Operating Parameters in the Energy Range of 20 to 80 MeV.

	CCL	BCDTL
No. of Tanks	86	86
Tank Length	5 $\beta\lambda$	5 $\beta\lambda$
Tank Diameter (cm)	32.23	25.4
No. of Cells/Tank	10	5
Cell Length	1/2 $\beta\lambda$	1 $\beta\lambda$
Intertank Spacing	3/2 $\beta\lambda$	2 $\beta\lambda$
Aperture Radius (cm)	2.5	2.0
ZT^2 (MΩ/m)	3.5 - 21.0	27.82- 34.28.
E_0T, Structure (MV/m)	1.3	1.3
φs (ramped)	-40° to -30°	-40° to -30°
Focusing Lattice	FODO	FODO
σ_0	80°	80°
Effective Quad Length (cm)	4.74	4.74
Quad. Gradients (KG/cm)	3.72 - 3.53	3.47 - 3.28

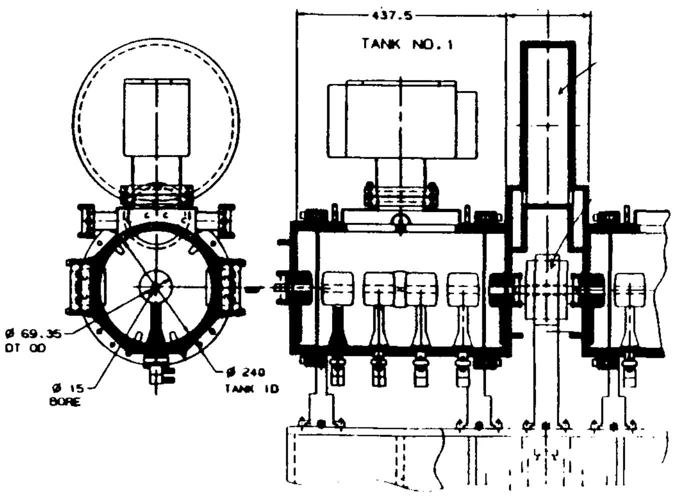

Fig. 3 BCDTL tank cutaway view showing the drift-tube geometry.

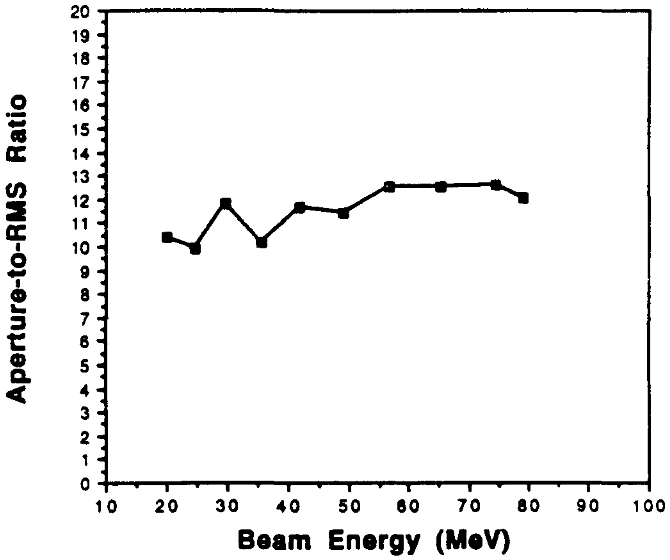

Fig. 5 Aperture to rms beam size ratio plotted as a function of beam energy along the BCDTL.

TABLE 2

Comparison of Simulation Results for the BCDTL and CCL Designs for APT/ATW at a Beam Current of I = 125 mA.

	CCL	BCDTL
$\varepsilon_{t,\,in}$ (π-cm-mrad)	0.024	0.024
$\varepsilon_{t,\,out}$ (π-cm-mrad)	0.024	0.026
$\varepsilon_{l,\,in}$ (π-deg-MeV)	0.21	0.21
$\varepsilon_{l,\,out}$ (π-deg-MeV)	0.26	0.29
a_o/x_{rms}	11-12	10-12

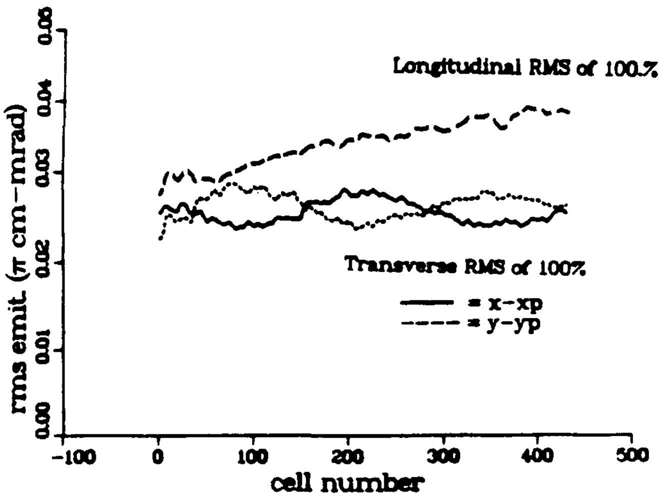

Fig. 4 Transverse and logitudinal emittances plotted as a function of cell number along the BCDTL.